Journal of Peptide Science
J. Pept. Sci. 2008; **14**: 510–517
Published online 12 November 2007 in Wiley InterScience (www.interscience.wiley.com). DOI: 10.1002/psc.954

JOURNAL OF PEPTIDE SCIENCE

Interfacial properties and structural analysis of the antimicrobial peptide NK-2[‡]

CLAUDIA OLAK,[a]* ANNABEL MUENTER,[a] JÖRG ANDRÄ[b] and GERALD BREZESINSKI[a]

[a] Max Planck Institute of Colloids and Interfaces, Research Campus Golm, Am Mühlenberg 1, 14476 Potsdam, Germany
[b] Research Center Borstel, Leibniz-Center for Medicine and Biosciences, Parkallee 10, 23845 Borstel, Germany

Received 22 June 2007; Revised 20 August 2007; Accepted 14 September 2007

Abstract: The structure of the antimicrobial peptide NK-2 has been studied at the air–water interface and in different solutions using spectroscopic methods such as circular dichroism (CD) and infrared reflection absorption spectroscopy (IRRAS) as well as specular X-ray reflectivity (XR). NK-2 adopts an unordered structure in water, buffer, and in the presence of monomeric cationic and noncharged amphiphiles. However, it forms a stable α-helix in 2,2,2-trifluoroethanol (TFE) and in micellar solutions of anionic, cationic as well as nonionic amphiphiles, whereas only in sodium dodecyl sulfonate solutions the α-helical structure can also be found below the critical micellar concentration (cmc). The amphiphilic molecule NK-2 is surface active and forms a Gibbs monolayer at the air–buffer interface. In contrast, no adsorption was observed if NK-2 is dissolved in water. During the adsorption process in buffer solutions, NK-2 undergoes a conformational transition from random coil in bulk to α-helix at the interface. This change of the peptide's secondary structure is known to be associated with its antimicrobial activity. A comparison of the experimental IRRA spectra with the simulated spectra indicates that the adsorbed NK-2 α-helix lies flat at the interface. This is confirmed by XR measurements which show that the thickness of the NK-2 layer is ~17 Å, which is the average diameter of a α-helix, indicating that only a monomolecular adsorption layer is formed.

Keywords: antimicrobial peptides; adsorption behavior; CD; IRRAS; X-ray reflectivity

INTRODUCTION

In the last decade, numerous publications have been devoted to antimicrobial peptides [1–7] isolated from a wide variety of bacteria, plants, insects, amphibians, and mammals including humans, and indicate a growing interest in these compounds. The current increase in resistance to conventional antibiotics and the high degree of selectivity possessed by antimicrobial peptides makes them suitable candidates for the development of alternatives to the classical antibiotics. Antimicrobial peptides are, in general, relatively small (<10 kDa), cationic, and adopt an amphipathic secondary structure upon membrane interaction. It is known that the conformational transitions of these biological macromolecules are ubiquitous and often of decisive importance to their biological function. These cationic peptides interact preferentially with acidic lipids which are particularly abundant in bacterial membranes. It has therefore been suggested that differences in the amount of acidic membrane phospholipids play a major role in sensitive cell specificity [8,9] Additionally, antimicrobial peptides bind to lipopolysaccharides on the outer membrane of gram-negative bacteria [10]. This interaction is a further example of peptide activation by membrane composition that leads to the disruption of bacteria's first barrier.

NK-2 (KILRGVCKKI MRTFLRRISK DILTGKK–NH_2) is an antimicrobial peptide derived from the cationic core region, representing the third and fourth helix (residues 39–65), of porcine NK-lysin. The sequence and the NMR-structure of NK-lysin are available in the literature [11,12]. The amphipathicity associated with this sequence makes the derived peptide NK-2 soluble in aqueous solution and promotes the formation of a mainly α-helical structure in membrane environments. NK-2 exerts a potent broad spectrum activity against bacteria (gram-positive and -negative) [13,14], fungi like *Candida albicans* [13], the protozoan parasite *Trypanosoma cruzi* [15], and also some cancer cells [16]. It shows low hemolytic activity and is devoid of cytotoxicity against human cell lines [13]. The interactions of NK-2 with phospholipids and lipopolysaccharides have been investigated using a range of methodologies, including fluorescence resonance energy transfer spectroscopy (FRET) [16], small-angle X-ray scattering (SAXS), differential scanning calorimetry (DSC) [17], and Fourier-transform infrared spectroscopy (FTIR) [18]. These techniques have shown that the target selectivity of NK–2 can be explained by a nonspecific higher affinity of the peptide for the cytoplasmic membrane lipid matrix of bacteria compared to human cells. NK–2 has a clear affinity for anionic charges, as expected

*Correspondence to: Claudia Olak, Max Planck Institute of Colloids and Interfaces, Am Mühlenberg 1, 14476 Potsdam, Germany;
e-mail: claudia.olak@mpikg.mpg.de
‡ This article is part of the Special Issue of the Journal of Peptide Science entitled "2nd workshop on biophysics of membrane-active peptides".

for a cationic peptide. Furthermore, the peptide has been shown to adopt an α-helical conformation in the presence of anionic lipids, contrary to the extended conformation of the peptide in solution. This conformational change is important in determining the mode of action of the peptide NK-2. The above described methods studied the interaction of the peptide with lipid-bilayer systems in solution. However, questions relating to the adsorption behavior at interfaces and the involved secondary structure changes remain to be studied. Lipid monolayers provide a flexible system to study interactions of the peptide with differently structured surfaces and allow observations of the behavior of NK-2 confined to a 2D environment [19]. The packing and charge density of phospholipid monolayers can be easily varied to study the effect of surface composition on peptide behavior. Representing one-half of a biological membrane, lipid monolayers can mimic membrane surfaces and are therefore ideal model systems to study the adsorption behavior or partial insertion of peptides into a lipid layer. Yet, before peptide–lipid interactions can be fully understood, the interfacial characteristics of the peptide alone must be clarified.

The aim of the present work is to study the surface properties of the peptide NK-2 by using the Langmuir-monolayer technique at the air–liquid interface. The structure and the orientation of NK-2 have been determined using infrared reflection absorption spectroscopy (IRRAS), a method used to study peptides *in situ* at the air–water interface. Specular X-ray reflectivity (XR) measurements have been performed to provide information on the adsorption layer on a molecular level. To complete the picture and to understand peptide behavior not only at interfaces, but also in solution, circular dichroism (CD) spectroscopy was used. To gain better insight into mechanisms of peptide adsorption, the peptide conformational behavior on different conditions has been analyzed by CD spectroscopy. Furthermore, the conformational properties of NK-2 when interacting with sodium dodecyl sulfonate (SDSF), cetyltrimethylammonium bromide (CTAB) and octylglucopyranoside (OG) monomers and micelles, as a membrane mimetic environment, were studied.

MATERIALS AND METHODS

Materials

The peptide NK-2 was synthesized with an amidated *C*-terminus and purified as described earlier [18]. The molecular weight is 3202 g/mol. The peptide, obtained as a solid powder, was dissolved to prepare stock solutions (1 g/l NK-2 in phosphate buffer; 10 mM, pH 7.3). SDSF was purchased from Sigma Aldrich, OG from Glycon Biochemicals, Luckenwalde, and CTAB and 2,2,2-trifluoroethanol (TFE) from Fluka. All solutions were prepared using Milli-Q deionized water (resistivity of 18.2 MΩ cm).

Circular Dichroism

Peptide secondary structure was examined by CD spectroscopy (Jasco J-715 CD spectrophotometer) using quartz cuvettes with an optical path length of 1 mm. The measurements were made using peptide concentration of 63 μM, and the peptide was added to the solutions directly before starting the measurement. All spectra were recorded at 25 °C. The spectra were measured in the wavelength interval from 190 to 300 nm with a 0.2-nm step resolution and a 1-nm bandwidth. The scanning rate was 50 nm/min with 2 s response time. The signal-to-noise ratio was improved by accumulating at least four scans. Data processing was carried out using the J-700 software package. The measured CD signal was transformed to mean residue molar ellipticity θ_R (deg cm^2/dmol). The blank spectra of the pure subphase (water, buffer, or TFE) were subtracted. To analyze the content of secondary structure elements, CONTIN (CONTIN/LL) method was used [20–22].

Peptide Adsorption

All adsorption experiments were performed in PTFE Langmuir troughs (Riegler & Kirstein, Potsdam, Germany). The surface pressure was measured by a Wilhelmy microbalance using a filter paper plate. The temperature of the subphase was maintained at $(20 \pm 0.5)^\circ$C. The trough was filled with pure water (Milli-Q, Millipore) or an aqueous buffer (10 mM phosphate buffer, pH 7.3) containing the peptide NK-2 in various concentrations. This type of preparation ensures a homogeneous distribution of the peptide. After filling the solution into the Langmuir trough, the surface was cleaned and the adsorption of the peptide was measured starting from a bare surface ($\pi = 0$ mN/m). The increase of surface pressure with time could be easily followed because of relatively slow NK-2 adsorption to the interface.

Infrared Reflection Absorption Spectroscopy

Infrared spectroscopy was used to determine the conformation and orientation of the adsorbed peptide. IRRA spectra were recorded on an IFS 66 FT-IR spectrometer (Bruker, Germany) equipped with a liquid nitrogen-cooled MCT (mercury cadmium telluride) detector. The spectrometer was coupled to a Langmuir-film balance, placed in a sealed container, to guarantee a constant-vapour atmosphere. The IR beam was conducted out of the spectrometer and focused onto the water surface of the Langmuir trough. A computer controlled rotating KRS-5 wire-grid polarizer (thallium bromide and iodide mixed crystal) was used to generate parallel (p) and perpendicular (s) polarized light. The angle of incidence was varied from 32° to 62° with respect to the surface normal. Measurements were performed using a trough with two connected compartments and a trough shuttle system [23]. One compartment contained the monolayer system under investigation (sample), whereas the other (reference) was filled with the pure subphase. The single-beam reflectance spectrum of the reference trough surface was ratioed as background to the single-beam reflectance spectrum of the sample to calculate the reflection absorption spectrum as $(-\log(R/R_0))$. IR spectra were collected at 8 cm^{-1} resolution using 200 scans for s-polarized light and 400 scans for p-polarized light. The mathematical model of Kuzmin *et al.* [24] and the formalism

DOI: 10.1002/psc

developed by Mendelsohn *et al.* [25] were applied to calculate IRRA spectra using the IDL software package. The IRRAS band intensities depend on the transition dipole moment orientation with respect to the surface plane. In the presented fits, the polar angles of the amide I and II bands were set to 30° and 90°, respectively. The real component of the refractive index and the polarizer efficiency used were 1.41 and 1%. All other parameters were chosen to best fit the experimental spectra.

Specular X-ray Reflectivity

Specular XR experiments were performed using the liquid-surface diffractometer on the undulator beamline BW1 at HASYLAB, DESY, Hamburg, Germany. The experimental setup and evaluation procedure have been described in detail elsewhere [26–28]. The Langmuir-film balance was thermostated (20 °C) and placed into a hermetically closed container filled with helium. The Langmuir trough was equipped with a single movable barrier and a Wilhelmy plate for monitoring the surface pressure. XR experiments reveal information on the electron-density distribution along the surface normal and may be used to determine the density and thickness of thin layers. The reflected intensity was measured by a NaI scintillation detector as a function of the vertical incidence angle, α_i, with the geometry $\alpha_i = \alpha_f = \alpha$, where α_f is the vertical exit angle of the reflected X-rays. An X-ray wavelength of $\lambda = 1.304$ Å was used. The vertical scattering vector component $q_z = (4\pi/\lambda)\sin\alpha_r$ was measured in a range between 0.01 and 0.85 Å^{-1}. The background scattering from, e.g. the subphase was measured at $2\theta_{hor} = 0.7°$ and subtracted from the signal measured at $2\theta_{hor} = 0°$. The reflectivity data were inverted by applying a model-independent approach. The obtained electron-density profile was interpreted by applying either a box model or assuming a symmetrical electron-density distribution.

RESULTS AND DISCUSSION

NK-2 Structure in Aqueous Solutions

Circular dichroism. The secondary structure of NK-2 in water, phosphate buffer, TFE (Figure 1), and in the presence of the differently charged amphiphiles (Figure 2) was determined by CD experiments. The content of secondary structure motifs determined by CONTIN/LL is summarized in Table 1.

CD spectra of the peptide in water and phosphate buffer (10 mM, pH 7.3) are typical for a random coil conformation (minimum at 198 nm). The quantitative determination of the secondary structure of NK-2 in water results in 2% α-helix, 23% β-sheet, 11% turn, and 64% random coil. In buffer, the values are 4% α-helix, 26% β-sheet, 12% turn, and 58% random coil. CD measurements were also performed with peptide in TFE solutions, to evaluate the propensity of NK-2 to adopt an α-helical conformation. Addition of fluoroalcohols, such as hexafluoroisopropanol or TFE, promotes the formation of α-helical structures. NK-2 displays a predominant α-helical structure in the presence of TFE (46% α-helix, 11% β-sheet, 15% turn, and 28% random coil). These results are in good agreement with those previously reported for this peptide under slightly different conditions by Andrä and Leippe [13].

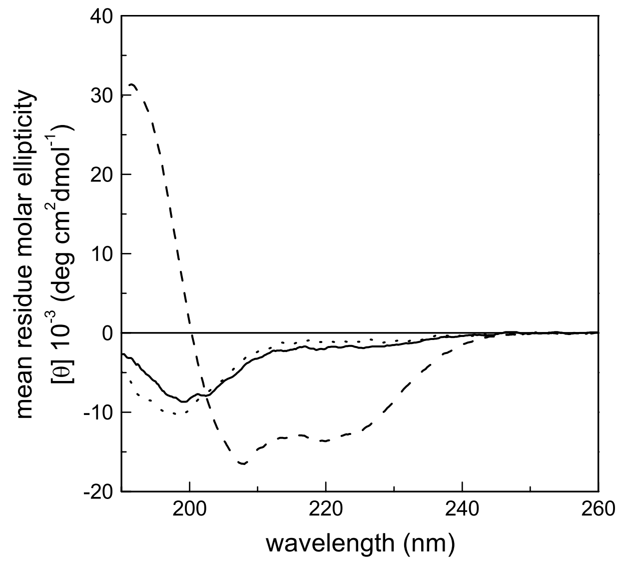

Figure 1 CD spectra (T∼25 °C) of NK-2 (63 µM) in phosphate buffer (solid line), in water (dotted line), and in TFE (dashed line).

Table 1 Secondary structure motif estimations for different NK-2 solutions obtained with the CONTIN/LL program (±3%) from CD data

Solution	Secondary structure motifs, %			
	α-helix	β-sheet	turn	random
water, pH 5.8	2	23	11	64
phosphate buffer, 10 mM, pH 7.3	4	26	12	58
TFE	46	11	15	28
SDSF monomers, 5 mM	43	15	15	27
SDSF micelles, 15 mM	44	10	16	30
CTAB monomers, 0.5 mM	4	27	15	54
CTAB micelles, 1.2 mM	18	26	17	39
OG monomers, 5 mM	5	35	14	46
OG micelles, 50 mM	31	17	21	32

The concentration-dependent effect of differently charged amphiphiles on the secondary structure of NK-2 was also characterized by CD (Figure 2). To study the effect of monomers and structured aggregates (micelles) on the secondary structure of NK-2, solutions were prepared with amphiphile concentrations below and above the critical micellar concentration (cmc). Figure 2(a) shows the CD spectra of NK-2 in the presence of SDSF monomers (5 mM) and micelles (15 mM). At both the concentrations, NK-2 exhibits a spectrum with the typical minima at 208 and

DOI: 10.1002/psc

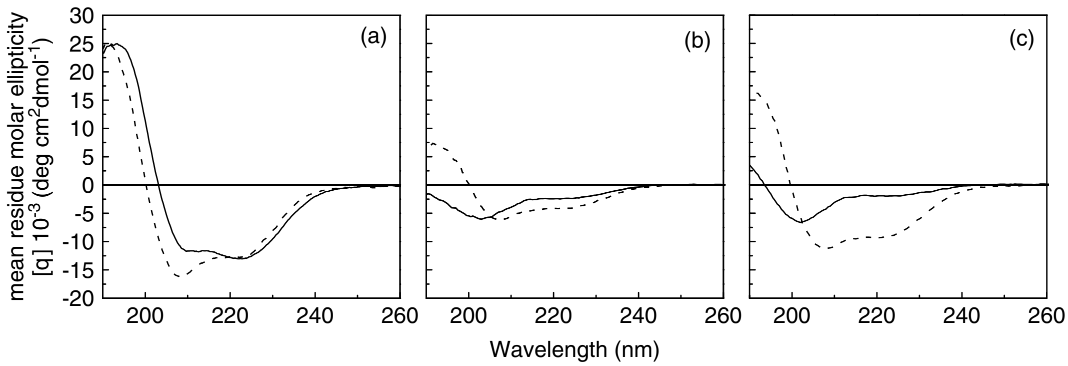

Figure 2 CD spectra (T~25 °C) of NK-2 (63 µM) in the presence of amphiphiles in monomeric and micellar concentrations. (a) Sodiumdodecylsulfonate, cmc = 10 mM: 5 mM (solid line) and 15 mM (dashed line); (b) Cetyltrimethylammonium bromide, cmc = 0.9 mM: 0.5mM (solid line) and 1.2 mM (dotted line); (c) Octylglucopyranoside, cmc = 25 mM: 5 mM (solid line) and 50 mM (dotted line).

222 nm, and a positive band at 190 nm, which is an indication of α-helical structure. Fitting the CD data led to 44% α-helix (Table 1) in both cases. At SDSF concentrations below the cmc (5 mM), the spectra contain less-pronounced bands when compared with the spectrum at 15 mM. This suggests that the α-helix content increased at higher concentrations of SDSF. In the case of cationic CTAB and nonionic OG solutions, the increase of the amphiphile concentration induces a clear conformational change of NK-2 from random coil at concentrations below the cmc to α-helix above the cmc. The measured CD spectra are shown in Figure 2(b) (CTAB) and 2(c) (OG). This results in a secondary structure motif content of 4% α-helix, 27% β-sheet, 15% turn, and 54% random coil in contact with CTAB monomers (0.5 mM) and 5% α-helix, 35% β-sheet, 14% turn, and 46% random coil in contact with OG monomers (5 mM). After the folding of NK-2 in the presence of micelles, the α-helix content amounts to 18% and 31% for 1.2 mM CTAB and 50 mM OG, respectively (Table 1). These two values are expected to be considerably higher. It should be noted that the software package used for the fitting of the measured CD spectra is optimized for the analysis of proteins and not small peptides. Thus, although the calculated results are unlikely to represent the absolute α-helical content of the peptide, they can be used for a relative comparison. In conclusion, our experiments show that below the cmc only anionic amphiphiles induce α-helical structure in NK-2. Cationic and nonionic amphiphile monomers have no influence on the peptide structure. The conformational transition of NK-2 from random coil to α-helix observed for SDSF is mainly a result of electrostatic interactions between the positively charged residues of the peptide and the negatively charged head of the amphiphile. In contrast, all amphiphiles were found to induce α-helix structure in NK-2 above the cmc. In this case, also hydrophobic interactions between the chains of the amphiphiles and the hydrophobic residues of NK-2 have to be taken into consideration. Apparently, the peptide penetrates partially into the micelle core (solubilization). This seems to be easily possible due to the dynamic equilibrium between surfactants in solution (monomers) and surfactants in aggregated form (micelles).

NK-2 Adsorption at the Air/Liquid Interface

Peptide adsorption. NK-2 is an amphiphatic peptide and has therefore a pronounced surface activity. The adsorption kinetics is concentration dependent and can be followed by using the Langmuir-film balance. The peptide was mixed with the subphase and adsorption started from a bare surface ($\pi = 0$ mN/m). Figure 3 (curve 1) and 4 show that the adsorption of NK-2 at the air/buffer interface leads to a surface pressure increase (decrease of surface tension). The adsorption kinetics is clearly concentration dependent. Increasing concentration leads to a faster adsorption process (Figure 4). The plateau in the plots corresponds to the saturation of the interface by the adsorbed peptide (adsorption and desorption are balanced). The maximum equilibrium surface pressure is 18 mN/m for an 1-µM peptide solution in PBS after about 2 h. The plateau values for curves 1–3 seem to be very similar, only the time course is different. This shows that a bulk concentration of 0.75 µM is already sufficient to allow a complete coverage of the surface by the peptide. The coverage is the limiting factor, so that any further concentration increase does not lead to an increased equilibrium pressure. In the case of curve 4 (0.5 µM), the adsorption process is very slow and the final equilibrium pressure might be already smaller than 18 mN/m. Therefore, the adsorption process of the peptide is similar to the behavior of common amphiphilic molecules. The peptide has a pronounced surface activity in phosphate buffer (10 mM, pH 7.3) but no adsorption is observed if NK-2 is dissolved in water (Figure 3, curve 2). This phenomenon was independently observed for other antimicrobial peptides such as melittin [29] and dicynthaurin [30]. By increasing the ionic strength with an injection of 100 mM KCl into water, the surface pressure immediately rises, which indicates an increased surface activity of NK-2. The pressure *versus* time curve exhibits a plateau at about 10 mN/m, which is below the expected value of the equilibrium surface pressure (18 mN/m) observed in buffer. Many proteins and peptides easily adsorb on Teflon surfaces, because hydrophobic side chains interact strongly with the surface. Therefore, the observed reduced equilibrium pressure is probably due to an exclusive adsorption of the peptide to the Teflon walls of the trough during the first 100 min of the experiment, resulting in a decrease of the effective peptide concentration.

Infrared reflection absorption spectroscopy. Adsorption of NK-2 and its secondary structure at the air/buffer interface were measured by IRRAS. During adsorption, amide and water bands appear and grow indicating an increased peptide concentration and layer density at the interface (Figure 5). The amide I band is associated mostly with the peptide C=O stretching vibration and the amide II band results from in-plane NH-bending and CN-stretching vibrations. The largest contribution in the amide I band region is observed at $\sim$1658 cm^{-1} and in the amide II region at $\sim$1546 cm^{-1}. Moreover, an amide A band occurs at $\sim$3260 cm^{-1} and is assigned to the amide stretching mode of the peptide backbone. The presence of an adsorbed peptide at the air/water interface leads to the appearance of the OH-stretching band at 3600 cm^{-1} and the H_2O-bending band in the region of the Amide bands (1700–1600 cm^{-1}). The intensity of these bands

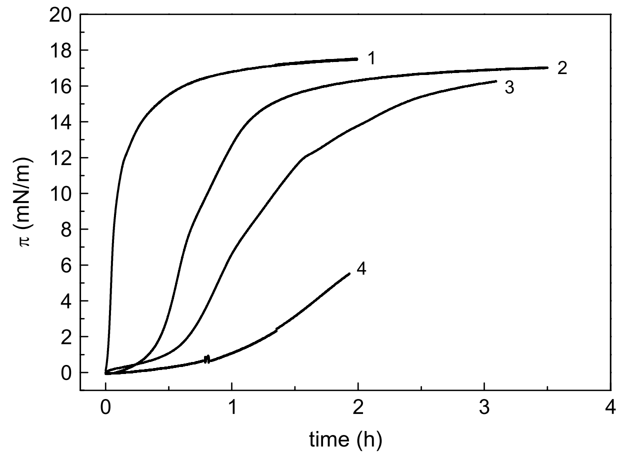

Figure 4 Adsorption kinetics at the air/buffer (phosphate buffer, 10 mM, pH 7.3) interface using different NK-2 concentrations: curve 1, 3 μM; curve 2, 1 μM; curve 3, 0.75 μM; curve 4, 0.5 μM.

depends on the effective adsorption-layer thickness [31], because the intensity of the water OH-stretch vibration in the spectrum of the sample trough is reduced in comparison with the reference trough since the adsorption layer replaces a water layer of the same thickness. An additional interesting observation is that upon compression of the peptide adsorption layer to surface pressures above the equilibrium value of 18 mN/m, the OH-stretching band increases (Figure 5). This can be only explained by either an unlikely increase of the peptide-layer thickness due to an out-of-plane tilting of the α-helices or an increased packing density in the peptide film due to an in-plane reorientation of the α-helices. In both the cases, this observation shows that the desorption kinetics is much slower than the adsorption kinetics.

The positions of the amide bands indicate that the peptide at the interface adopts either an α-helical or a

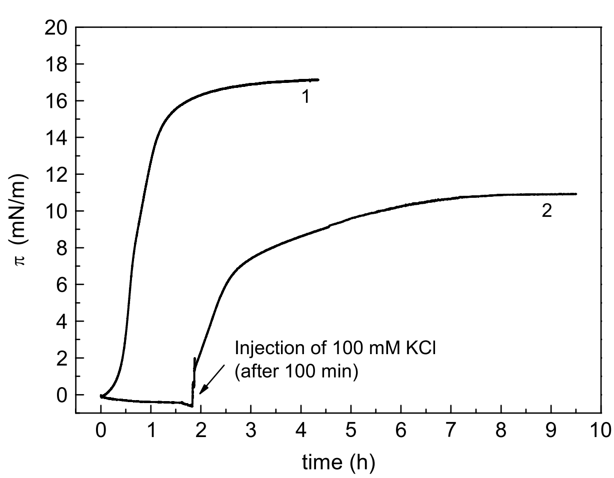

Figure 3 Adsorption of NK-2 to the air/liquid interface. The peptide (peptide bulk concentration = 1 μM) dissolved in phosphate buffer (10 mM, pH 7.3) (curve 1), and in water (curve 2) at 20 °C. Injection of 100 mM KCl (NK-2 in water) after 100 min.

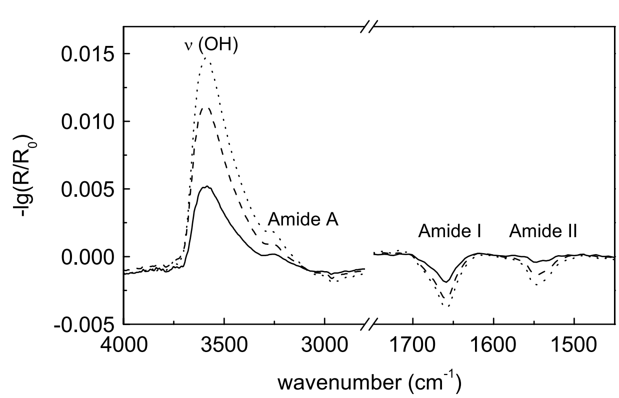

Figure 5 IRRA spectra of NK-2 adsorbed to the air/buffer interface at 17.1 mN/m (solid line), and after compression to 30.1 mN/m (dashed line) and 39.9 mN/m (dotted line). Spectra have been recorded at an angle of incidence of 40° and with s-polarized light.

DOI: 10.1002/psc

random coil conformation [32]. Measurements at different angles of incidence using different polarizations of the incident light can help to distinguish between these two conformations. Therefore, measurements using p-polarized light at different angles of incidence have been performed. For s-polarized light, the absolute values of the band intensity in the reflectance absorbance spectrum increase monotonically with increasing angle of incidence and therefore do not allow obtaining detailed information about the anisotropy of the film. The reason for this is that s-polarized light probes only the dipole moment component parallel to the surface, whereas p-polarized light probes the dipole moment components parallel and perpendicular to the surface. For p-polarized light the sign of the band changes at the Brewster angle and the resulting changes in band direction, intensity, and position allow the determination of orientations of secondary structure elements. To elucidate the NK-2 conformation and orientation at the interface, measured IRRA spectra can be compared with simulated spectra. Figure 6 illustrates the IRRA spectra of the amide regions for the pure peptide monolayer measured at different angles of incidence. The spectra can be best described by an α-helix with its helical axis in the surface plane. The extinction coefficients of the peaks were chosen to best fit the experimental data. The determined values, $k_{\max}(\text{amide I}) = 1.5$ and $k_{\max}(\text{amide II}) = 0.7$, are in good agreement with literature values [33,34]. The simulated spectra are in very good agreement with the experimental IRRA spectra. Therefore, the comparison of measured spectra with simulated ones indicates that NK-2 forms an α-helix, oriented parallel to the interface.

In conclusion, using IRRA spectra acquired with p-polarized light at various angles of incidence shows that the peptide adsorbed at the interface forms an α-helix, although the peptide has a predominantly random coil conformation in water and in buffer, as proved by CD spectroscopy.

Specular X-ray reflectivity. For XR measurements, the NK-2 adsorption layer at the air–buffer interface has been formed as described above. Grazing incidence X-ray diffraction (GIXD) measurements were also performed, but no diffraction peaks were observed, indicating the lack of any in-plane ordering within the adsorption layer. The XR data and the corresponding electron-density profile for a compressed NK-2 adsorption layer are shown in Figure 7. Unfortunately, a precise determination of the pressure was not possible. The peptide film is very stiff, so that the Wilhelmy plate starts to tilt upon compression using only one movable barrier. The reflectivity profile of NK-2 can be fitted by an one-box model with a thickness of (16.9 ± 0.2) Å and an electron density of (0.424 ± 0.02) e$^-$/Å^3. The roughness of the subphase-peptide surface is (4.2 ± 0.1) Å and that of the peptide-air surface is (3.0 ± 0.1) Å. The layer thickness of ~17 Å agrees well with the

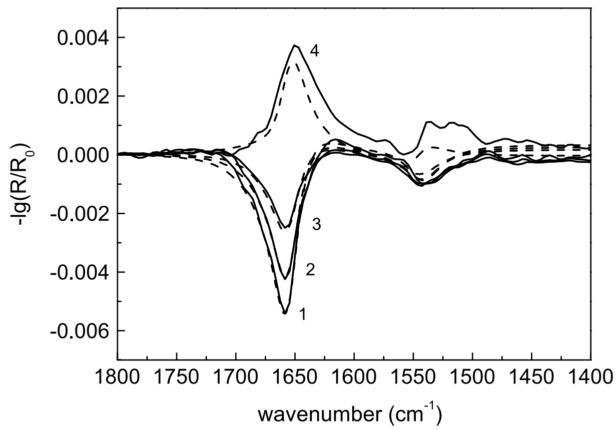

Figure 6 Comparison of experimental IRRA spectra of NK-2 adsorption to the air/buffer interface (solid lines) with simulations of IRRA spectra (dashed lines). The peptide concentration was 1 μM; the final surface pressure was 17.4 mN/m. Spectra were acquired with s-polarized light at 40° (3) and p-polarized light at various angles of incidence 40° (1), 30° (2), and 60° (4). The experimental spectra were not baseline corrected but shifted vertically to zero at 1800 cm^{-1}. The full width at half-maximum, fwhm (35 for amide I and 40 for amide II) and extinction coefficients of the peaks were chosen to best fit the experimental data. The effective thickness of the monolayer was chosen to be 10 Å based on fits to the height of the OH-stretching band in the IRRA spectra at 3600 cm^{-1}.

average diameter of an α-helix described in the literature [35–37]. Combining the results of IRRAS and XR measurements, it is shown that NK-2 adsorbs as a monomolecular layer of α-helices lying flat at the interface.

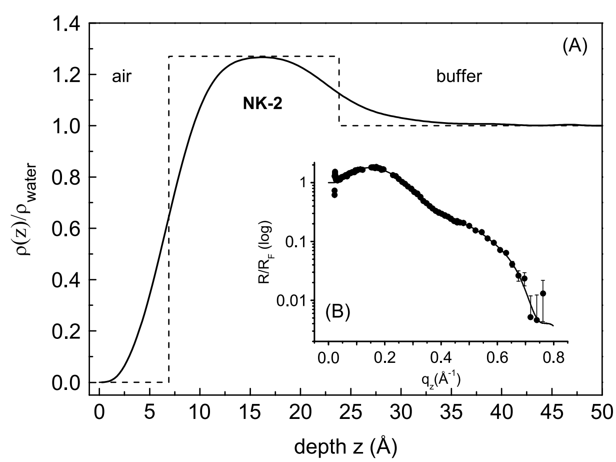

Figure 7 Specular X-ray reflectivity normalized by the Fresnel-reflectivity, R/RF vs. qz (inset B), and the corresponding electron-density profile (solid line in A) of NK-2 adsorbed at the air/buffer interface. The dashed lines represent the one-box model used to describe the electron-density profile. Solid line in panel B is the best fit using a model-independent approach. The peptide concentration was 1 μM; the monolayer was highly compressed.

DOI: 10.1002/psc

CONCLUSIONS

The presented studies of the surface active antimicrobial peptide NK-2 in solution under different environmental perturbations and at the air–liquid interface show the following results:

1. NK-2 adopts an unordered structure in water, buffer, and in the presence of monomeric cationic and noncharged amphiphiles.
2. The peptide forms a stable α-helix in TFE, in monomeric SDSF and in micellar solutions of different amphiphiles.
3. NK-2 undergoes a conformational transition from random coil to α-helical structure during the adsorption from bulk system to the air–buffer interface. Since the peptide layer can be compressed to pretty high surface pressures, the desorption kinetics must be very slow, which can be understood in terms of a trapping of the α-helix at the interface.
4. The orientation and the geometrical dimension of the helix at the interface can be successfully monitored by IRRAS and XR. After adsorption to a bare buffer surface IRRA spectra show that the NK-2 lies flat, with the helix long axis parallel to the interface. This is in line with the measured total thickness of the NK-2 adsorption layer ($\sim$17 Å).

In summary, the present work describes the conformational transition of NK-2 during the adsorption process from a bulk solution to the air/liquid interface. This adsorption of the amphiphatic peptide is strongly influenced by the subphase bulk composition. Variables such as concentration, ionic strength, pH, and temperature have to be taken into account to analyze the surface activity associated with conformational factors. The investigations of antimicrobial peptides in bulk and at the interface are essential to understand the conformational characteristics of these molecules. Many antimicrobial peptides studied in the recent years are known to adopt an α-helical structure in the presence of membranes, and the importance of this structure for antimicrobial activity has been a subject of debate. Nevertheless, the structural changes of these peptides, especially without the influence of additional lipids, are rarely investigated, yet can be helpful for learning more about the mode of action of these possible alternatives to classical antibiotics.

Acknowledgements
We gratefully acknowledge beamtime at HASYLAB, DESY (Hamburg, Germany) and Dr K. Kjaer for his valuable help with the beamline setup.

REFERENCES

1. Bevins CL, Zasloff M. Peptides from Frog-Skin. *Annu. Rev. Biochem.* 1990; **59**: 395–414.
2. Boman HG. Peptide antibiotics and their role in innate immunity. *Ann. Rev. Immunol.* 1995; **13**: 61–92.
3. Broekaert WF, Cammue BPA, DeBolle MFC, Thevissen K, DeSamblanx GW, Osborn RW. Antimicrobial peptides from plants. *Crit. Rev. Plant Sci.* 1997; **16**: 297–323.
4. Hancock REW, Lehrer R. Cationic peptides: a new source of antibiotics. *Trends Biotechnol.* 1998; **16**: 82–88.
5. Katz E, Demain AL. Peptide antibiotics of bacillus – chemistry, biogenesis, and possible functions. *Bacteriol. Rev.* 1977; **41**: 449–474.
6. White SH, Wimley WC, Selsted ME. Structure, function, and membrane integration of defensins. *Curr. Opin. Struct. Biol.* 1995; **5**: 521–527.
7. Zasloff M. Antimicrobial peptides of multicellular organisms. *Nature* 2002; **415**: 389–395.
8. Matsuzaki K, Sugishita K, Fujii N, Miyajima K. Molecular-basis for membrane selectivity of an antimicrobial peptide, magainin-2. *Biochemistry* 1995; **34**: 3423–3429.
9. Schröder-Borm H, Willumeit R, Brandenburg K, Andrä J. Molecular basis for membrane selectivity of NK-2, a potent peptide antibiotic derived from NK-lysin. *Biochim. Biophys. Acta* 2003; **1612**: 164–171.
10. Piers KL, Brown MH, Hancock REW. Improvement of outer membrane-permeabilizing and lipopolysaccharide-binding activities of an antimicrobial cationic peptide by C-terminal modification. *Antimicrob. Agents Chemother.* 1994; **38**: 2311–2316.
11. Andersson M, Gunne H, Agerberth B, Boman A, Bergman T, Sillard R, Jornvall H, Mutt V, Olsson B, Wigzell H, Dagerlind A, Boman HG, Gudmundsson GH. Nk-lysin, a novel effector peptide of cytotoxic T-cells and Nk-cells – structure and cDNA cloning of the porcine form, induction by interleukin-2, antibacterial and antitumor-activity. *Embo J.* 1995; **14**: 1615–1625.
12. Liepinsh E, Andersson M, Ruysschaert JM, Otting G. Saposin fold revealed by the NMR structure of NK-lysin. *Nat. Struct. Biol.* 1997; **4**: 793–795.
13. Andrä J, Leippe M. Candidacidal activity of shortened synthetic analogs of amoebapores and NK-lysin. *Med. Microbiol. Immunol.* 1999; **188**: 117–124.
14. Andrä J, Monreal D, de Tejada GM, Olak C, Brezesinski G, Gomez SS, Goldmann T, Bartels R, Brandenburg K, Moriyon I. Rationale for the design of shortened derivatives of the NK-lysin-derived antimicrobial peptide NK-2 with improved activity against gram-negative pathogens. *J. Biol. Chem.* 2007; **282**: 14719–14728.
15. Jacobs T, Bruhn H, Gaworski I, Fleischer B, Leippe M. NK-lysin and its shortened analog NK-2 exhibit potent activities against Trypanosoma cruzi. *Antimicrob. Agents Chemother.* 2003; **47**: 607–613.
16. Schröder-Borm H, Bakalova R, Andrä J. The NK-lysin derived peptide NK-2 preferentially kills cancer cells with increased surface levels of negatively charged phosphatidylserine. *FEBS Lett.* 2005; **579**: 6128–6134.
17. Willumeit R, Kumpugdee M, Funari SS, Lohner K, Navas BP, Brandenburg K, Linser S, Andra J. Structural rearrangement of model membranes by the peptide antibiotic NK-2. *Biochim. Biophys. Acta* 2005; **1669**: 125–134.
18. Andrä J, Koch MHJ, Bartels R, Brandenberg K. Biophysical characterization of endotoxin inactivation by NK-2, an antimicrobial peptide derived from mammalian NK-lysin. *Antimicrob. Agents Chemother.* 2004; **48**: 1593–1599.
19. Maget-Dana R. The monolayer technique: a potent tool for studying the interfacial properties of antimicrobial and membrane-lytic peptides and their interactions with lipid membranes. *Biochim. Biophys. Acta* 1999; **1462**: 109–140.

20. Greenfield NJ. Methods to estimate the conformation of proteins and polypeptides from circular dichroism data. *Anal. Biochem.* 1996; **235**: 1–10.
21. Provencher SW, Glockner J. Estimation of globular protein secondary structure from circular-dichroism. *Biochem.* 1981; **20**: 33–37.
22. Sreerama N, Venyaminov SY, Woody RW. Estimation of protein secondary structure from circular dichroism spectra: inclusion of denatured proteins with native proteins in the analysis. *Anal. Biochem.* 2000; **287**: 243–251.
23. Flach CR, Gericke A, Mendelsohn R. Quantitative determination of molecular chain tilt angles in monolayer films at the air/water interface: Infrared reflection/absorption spectroscopy of behenic acid methyl ester. *J. Phys. Chem. B* 1997; **101**: 58–65.
24. Kuzmin VL, Mikhailov AV. Molecular theory of light-reflection and the applicability limits of a macroscopic approach. *Opt Spektrosk.* 1981; **51**: 691–695.
25. Mendelsohn R, Brauner JW, Gericke A. External infrared reflection-absorption spectrometry monolayer films at the air-water-interface. *Annu. Rev. Phys. Chem.* 1995; **46**: 305–334.
26. Jensen TR, Balashev K, Bjoernholm T, Kjaer K. Novel methods for studying lipids and lipases and their mutual interaction at interfaces. Part II. Surface sensitive synchrotron X-ray scattering. *Biochimie.* 2001; **83**: 399–408.
27. Kaganer VM, Brezesinski G, Möhwald H, Howes PB, Kjaer K. Positional order in Langmuir monolayers: an x-ray diffraction study. *Phys. Rev. E* 1999; **59**: 2141–2152.
28. Rietz R, Rettig W, Brezesinski G, Bouwman WG, Kjaer K, Möhwald H. Monolayer behaviour of chiral compounds at the air-water interface: 4-hexadecyloxy-butane-1,2-diol. *Thin Solid Films* 1996; **285**: 211–215.
29. Blaudez D, Turlet JM, Dufourcq J, Bard D, Buffeteau T, Desbat B. Investigations at the air/water interface using polarization modulation IR spectroscopy. *J. Chem. Soc., Faraday Trans.* 1996; **92**: 525–530.
30. Bringezu F, Majerowicz M, Maltseva E, Wen S, Brezesinski G, Waring AJ. Penetration of the antimicrobial peptide dicynthaurin into phospholipid monolayers at the liquid-air interface. *ChemBioChem* 2007; **8**: 1038–1047.
31. Meister A, Kerth A, Blume A. Interaction of sodium dodecyl sulfate with dimyristoyl-sn-glycero-3-phosphocholine monolayers studied by infrared reflection absorption spectroscopy. A new method for the determination of surface partition coefficients. *J. Phys. Chem. B* 2004; **108**: 8371–8378.
32. Kalnin NN, Baikalov IA, Venyaminov SY. Quantitative Ir spectrophotometry of peptide compounds in water (H_2O) solutions. 3. Estimation of the protein secondary structure. *Biopolymers* 1990; **30**: 1273–1280.
33. Buffeteau T, Le Calvez E, Castano S, Desbat B, Blaudez D, Dufourcq J. Anisotropic optical constants of alpha-helix and beta-sheet secondary structures in the infrared. *J. Phys. Chem. B* 2000; **104**: 4537–4544.
34. Dyck M, Kerth A, Blume A, Losche M. Interaction of the neurotransmitter, neuropeptide Y, with phospholipid membranes: infrared spectroscopic characterization at the air/water interface. *J. Phys. Chem. B* 2006; **110**: 22152–22159.
35. Ambroggio EE, Separovic F, Bowie J, Fidelio GD. Surface behaviour and peptide-lipid interactions of the antibiotic peptides, Maculatin and Citropin. *Biochim. Biophys. Acta* 2004; **1664**: 31–37.
36. Vie V, Van Mau N, Chaloin L, Lesniewska E, Le Grimellec C, Heitz F. Detection of peptide-lipid interactions in mixed monolayers, using isotherms, atomic force microscopy, and Fourier transform infrared analyses. *Biophys. J.* 2000; **78**: 846–856.
37. Zagrovic B, Jayachandran G, Millett IS, Doniach S, Pande VS. How large is an alpha-helix? Studies of the radii of gyration of helical peptides by small-angle X-ray scattering and molecular dynamics. *J. Mol. Biol.* 2005; **353**: 232–241.